Spin Relaxation of Conduction Electrons in Polyvalent Metals: Theory and a Realistic Calculation

J. Fabian and S. Das Sarma
Department of Physics, University of Maryland at College Park, College Park, Maryland 20742-4111
(Received 13 July 1998)

Relaxation of electronic spins in metals is significantly enhanced whenever a Fermi surface crosses Brillouin zone boundaries, special symmetry points, or lines of accidental degeneracy. A realistic calculation shows that if aluminum had one valence electron its spin relaxation would be slower by nearly 2 orders of magnitude. This not only solves a long-standing experimental puzzle, but also provides a way of tailoring spin dynamics of electrons in a conduction band. [S0031-9007(98)08021-1]

PACS numbers: 71.70.Ej, 75.40.Gb, 76.30.Pk

Electronic spin is emerging as a building block of new digital devices. The all-metal bipolar spin transistor [1] was already demonstrated and new devices are being built using the phenomenon of giant magnetoresistance [2]. Recent advances in spin-coherent dynamics in semiconductors [3] may advance the development of a quantum computer [4]. All of these new technological applications rely on a relatively long relaxation time of conduction electron spin eigenstates. In this Letter, we consider theoretically the problem of electronic spin relaxation in metals, and solve an outstanding puzzle, explaining why very similar metals (for example, Al and Na) may have spin relaxation rates differing by 2 or 3 orders of magnitude.

Experiments [5,6] show that spin states in metals live several orders of magnitude longer than momentum states. Furthermore, unlike momentum relaxation times τ, spin relaxation times T_1 [7] vary significantly among metals. According to Elliott [8] and Yafet [9], two factors cause electronic spin in metals to decay: (i) the spin-orbit interaction induced, for example, by (crystal) ions or impurities, and (ii) a momentum relaxation process such as impurity or phonon scattering. The product c^2T_1, where c^2 is a measure of the strength of the spin-orbit interaction, is then well approximated by τ and has similar magnitude for all simple metals. Considering only ion-induced spin-orbit interaction, crystalline and atomic c^2 should be similar. Indeed, by substituting the atomic values for c^2, Monod and Beuneu [10] found a "Grüneisen" behavior of c^2T_1 for all alkali and noble metals: as a function of reduced temperature T/T_D, where T_D is a Debye temperature, the values of c^2T_1 fall onto a single curve. On the other hand, metals Al, Pd, Mg, and Be have c^2T_1 much smaller (up to 3 orders of magnitude for Mg and Be) than the "main group." For example, the atomic c^2 for aluminum differs by less than 10% from that for sodium [10], yet the spin relaxation times at Debye temperatures are 0.1 ns for aluminum [11] ($T_D = 394$ K [12]) and 20 ns for sodium [5,13] ($T_D = 150$ K [12]); the corresponding momentum relaxation times are in the ratio 1:7 [14]. We resolve this puzzle by showing that the crystalline c^2 is about 30 times greater in Al than in Na due to a rather subtle "band renormalization" effect.

In this paper, we answer why spin in some metals decays unexpectedly fast, by introducing the concept of *band renormalized* spin-orbit interaction strength c^2. Common to the "strange" metals (Al, Pd, Mg, and Be) with unusually fast spin relaxation is that their Fermi surfaces contain regions where c^2 is significantly enhanced. Such regions are found near Brillouin zone (BZ) boundaries, special symmetry points, or lines of accidental degeneracy. Although these spin "hot spots" comprise, generally, only a small part of the Fermi surface, they almost entirely determine the effective value of c^2. We predict that the strange behavior is, in fact, common to all polyvalent metals, where spin hot spots are a consequence of the Fermi surface topology. This prediction is particularly significant since no polyvalent metals other than Al, Pd, Mg, and Be have been measured for T_1 so far. Furthermore, our calculations show that T_1 can be appreciably altered by modifying the band structure (by alloying, doping, reducing the dimensionality, etc.). Our prediction is based on a realistic pseudopotential calculation for aluminum and analytical estimates for c^2.

If the periodic potential due to ions in a crystal lattice contains spin-orbit coupling (a term proportional to the scalar product of the orbital and spin momentum operators, $\hat{\mathbf{L}} \cdot \hat{\mathbf{S}}$), the electronic Bloch states are a mixture of spin up $|\uparrow\rangle$ and down $|\downarrow\rangle$ species [8]: $\Psi^{\uparrow}_{\mathbf{k}n}(\mathbf{r}) = [a_{\mathbf{k}n}(\mathbf{r})\ |\uparrow\rangle + b_{\mathbf{k}n}(\mathbf{r})\ |\downarrow\rangle]\exp(i\mathbf{k}\cdot\mathbf{r})$ and $\Psi^{\downarrow}_{\mathbf{k}n}(\mathbf{r}) = [a^{*}_{-\mathbf{k}n}(\mathbf{r})\ |\downarrow\rangle - b^{*}_{-\mathbf{k}n}(\mathbf{r})\ |\uparrow\rangle]\exp(i\mathbf{k}\cdot\mathbf{r})$. The lattice momentum $\mathbf{k}$ is confined to the first BZ, n is a band index, and $a_{\mathbf{k}n}(\mathbf{r})$ and $b_{\mathbf{k}n}(\mathbf{r})$ are complex periodic functions with the period of the lattice: if $\mathbf{G}$ denotes the reciprocal lattice vectors, then $a_{\mathbf{k}n}(\mathbf{r}) = \sum_{\mathbf{G}} a_{\mathbf{k}n}(\mathbf{G})\exp(i\mathbf{G}\cdot\mathbf{r})$ and similarly for $b_{\mathbf{k}n}(\mathbf{r})$. Both states have the same energy $E_{\mathbf{k}n}$, as follows from time and space inversion symmetry [8]; the numbering of bands is therefore the same as without the spin notation. The degenerate states $\Psi^{\uparrow}_{\mathbf{k}n}$ and $\Psi^{\downarrow}_{\mathbf{k}n}$ are chosen to represent electrons with spins polarized along the z direction [9]: $(\Psi^{\downarrow}_{\mathbf{k}n}|\hat{S}_z|\Psi^{\downarrow}_{\mathbf{k}n}) = -(\Psi^{\uparrow}_{\mathbf{k}n}|\hat{S}_z|\Psi^{\uparrow}_{\mathbf{k}n}) < 0$ and

 0031-9007/98/81(25)/5624(4)$15.00

the off-diagonal matrix elements are zero. This condition implies that $a_{\mathbf{k}n}(\mathbf{r})$ have values close to one, while $b_{\mathbf{k}n}(\mathbf{r})$ are much smaller, decreasing with the decrease of the strength of the spin-orbit interaction (with the exception of the points where the spin-orbit interaction lifts a degeneracy).

Elliott [8] noticed that ordinary (spin conserving) impurity or phonon scattering can induce transitions between $\Psi^{\uparrow}_{\mathbf{k}n}$ and $\Psi^{\downarrow}_{\mathbf{k}'n'}$, leading to the flip of a spin polarization and thus spin relaxation. If $\langle b^2\rangle$ is the Fermi surface average of $|b_{\mathbf{k}n}|^2 = \sum_{\mathbf{G}} |b_{\mathbf{k}n}(\mathbf{G})|^2$, spin relaxation rate $1/T_1 \approx 4\langle b^2\rangle (1/\tau)$ (that is, $c^2 \approx 4\langle b^2\rangle$). Such a formula could be obtained by assuming that (i) $1/\tau \gg 1/T_1$ [15], (ii) $a_{\mathbf{k}n}(\mathbf{r}) \approx 1$, (iii) the scattering form factor has a constant amplitude, and (iv) the interference between $b_{\mathbf{k}n}(\mathbf{G})$ with different $\mathbf{G}$ is neglected. Assumptions (i) and (ii) are usually satisfied. Assumption (iii) implies a scattering by a delta-function-like impurity potential. This simplification is consistent with our goal to establish the effect of band structure (through $b_{\mathbf{k}n}$) on T_1 rather than to study particular scattering processes. The neglect of interference can be justified if the scattering form factors have a rapidly varying phase. Although such a form factor [that also satisfies (iii)] is hardly found, realistic form factors do oscillate on the momentum scale where the transitions occur. Assumption (iv) is then partly justified, since the phase attached to $b_{\mathbf{k}n}(\mathbf{G})$ will be different for different $\mathbf{G}$.

The spin-mixing parameters $|b_{\mathbf{k}n}|^2$ can have a broad range of values, depending on the position of $\mathbf{k}$ in the BZ. Consider a band structure computed without the spin-orbit interaction. If the closest band to n is separated from n by Δ, the spin-orbit interaction mixes the spins from the two bands (direct interband transitions): $|b_{\mathbf{k}n}|^2 \approx (1 - \Delta/\sqrt{\Delta^2 + 4V_{\mathrm{SO}}^2})/2$, where V_{SO} is some effective spin-orbit interaction. Three cases occur. (A) For a general point, the band separation is of order E_F, the Fermi energy, so that $\Delta \gg V_{\mathrm{SO}}$ and $|b_{\mathbf{k}n}|^2 \approx (V_{\mathrm{SO}}/E_F)^2$. (B) If the state is close to a BZ plane that cuts $\mathbf{G}$ by half, the band separation is $\approx 2V_{\mathbf{G}}$ ($V_{\mathbf{G}}$ is the $\mathbf{G}th$ Fourier coefficient of the nonspin part of the lattice potential). Since typically $V_{\mathbf{G}} \gg V_{\mathrm{SO}}$, $|b_{\mathbf{k}n}|^2 \approx (V_{\mathrm{SO}}/2V_{\mathbf{G}})^2$; this can be a few orders larger than in (A). Finally, (C) the spin-orbit interaction can lift the degeneracy of two or more bands. The mixing of spins is complete and $|b_{\mathbf{k}n}|^2 \approx |a_{\mathbf{k}n}|^2 \approx 0.5$. The states with property (C) are not covered by the Elliott-Yafet theory [9]. This is not a concern, however, since, as we show below, such states are statistically irrelevant for aluminum T_1.

To illustrate how the band structure affects $\langle b^2\rangle$ (and T_1), we perform a pseudopotential calculation for aluminum, where all three cases (A) to (C) occur. Our pseudopotential has a nonspin (scalar) part and a spin-orbit term. The scalar part [16] has the nice feature [in view of estimate (B)] of being fitted to the experimental values [17] of $V_1 = V_{111} = 0.008\,95$ a.u. and $V_2 = V_{200} = 0.0281$ a.u. (1 a.u. = 2 Ry). In addition to accurately reproducing the band structure of aluminum, this form factor gives reasonable results [16] for the resistivity of liquid aluminum, making it useful in scattering problems. The spin-orbit part of our pseudopotential is $\lambda \hat{\mathbf{L}} \cdot \hat{\mathbf{S}} \mathcal{P}_l$, where $\mathcal{P}_l$ is the operator projecting on the orbital momentum state l. The parameter $\lambda = 2.7 \times 10^{-3}$ a.u. inside the ion core of twice the Bohr radius, $r_c = 2r_B$. Outside the core λ vanishes. This estimate for λ is based on the first-principles spin-orbit pseudopotential of Ref. [18]. Since the spin-orbit interaction acts only inside the core, the effective V_{SO} is reduced to about $(r_c^3/V_a)\lambda$ ($\approx \lambda/10$ for aluminum, where the primitive cell volume $V_a \approx 111 r_B^3$).

Having the band structure, the challenge is to evaluate the average of $|b_{\mathbf{k}n}|^2$, a quantity that varies over several orders of magnitudes. We do the averaging by the tetrahedron method [19] with a carefully designed grid that envelops the two sheets of the aluminum Fermi surface (bands 2 and 3). The grid is denser in the regions where Δ is smaller (around BZ boundaries and accidental degeneracy points). This adaptation of the grid is necessary to ensure that $|b_{\mathbf{k}n}|^2$ can be linearly interpolated inside the grid cells (tetrahedrons), as assumed in the tetrahedron method. The number of grid points (in the irreducible wedge of the first BZ) where the band-structure equations must be solved is about ten thousand.

Figure 1 plots the calculated distribution ρ of the values attainable by $|b_{\mathbf{k}n}|^2$ over the Fermi surface (the visual perspective of the distribution is in Fig. 2). The span is enormous—almost seven decades. The majority of states have $|b_{\mathbf{k}n}|^2$ below 10^{-5}. These are the generic points from the estimate (A). Once the Fermi surface approaches the BZ planes (violet in Fig. 2), the values jump to 10^{-5}–10^{-4}. However, the largest $|b_{\mathbf{k}n}|^2$ are found near the accidental degeneracy points R (red spots in Fig. 2); these points do not lie on symmetry lines, yet they have

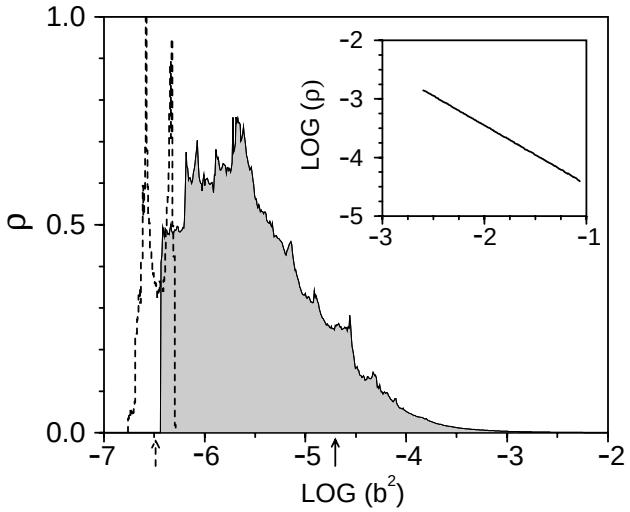

FIG. 1. Calculated distribution ρ (in arbitrary units) of the spin-mixing parameters $|b_{\mathbf{k}n}|^2$ for aluminum. The corresponding average $\langle b^2\rangle \approx 2.0 \times 10^{-5}$ is indicated by a solid arrow. The linear tail of the distribution is shown in the inset. The dashed line shows what the distribution would be if aluminum were monovalent ($\langle b^2\rangle \approx 3.4 \times 10^{-7}$, dashed arrow).

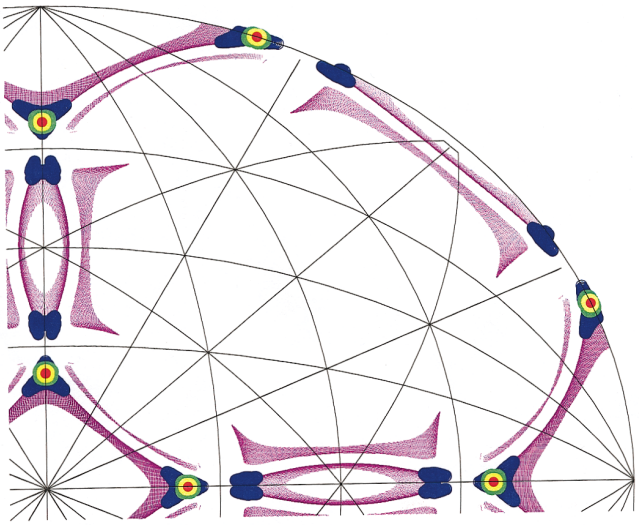

FIG. 2(color). Stereogram of the Fermi momentum directions in aluminum. The fragment shows the spin hot spots: the points $\mathbf{k}$ (in an extended-zone scheme) with $|b_{\mathbf{k}n}|^2 \geq 10^{-5}$. Colors violet, blue, green, yellow, and red indicate a successive increase of b^2: violet points have b^2 from 10^{-5} to 10^{-4}; blue 10^{-4} to 10^{-3}; etc., up to 10^{-1} to 1 for red. To improve their visibility, the weight of the colors (except for violet) is enhanced.

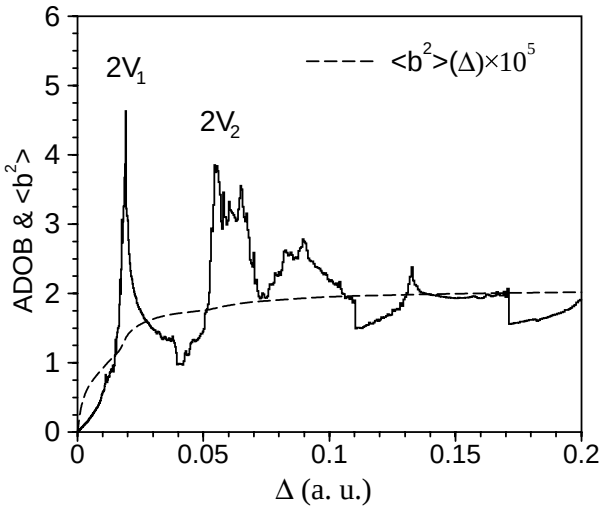

FIG. 3. Calculated average density of bands (ADOB) and cumulative average spin-mixing parameter $\langle b^2\rangle(\Delta)$ for aluminum.

degenerate bands [20] if no spin-orbit interaction is present. The spin-orbit interaction lifts this degeneracy and completely mixes the spin states as in the estimate (C). The unusually long tail of ρ ensures the large value of the average $\langle b^2\rangle \approx 2.0 \times 10^{-5}$, about 10 times larger than the value where ρ is maximal. To ensure that the above picture is valid for a large temperature range, we checked that spin hot spots survive energy excitations of at least $\approx kT_D$ ($\approx$35 meV) above and below the Fermi surface. This also invalidates the objection that small relativistic corrections (of a few meV) could affect the existence of the spin hot spots in aluminum.

The band structure role in $\langle b^2\rangle$ becomes even more evident from the plot (Fig. 1) of ρ for a hypothetical case of monovalent aluminum (the lattice and the form factors are unchanged). The monovalent aluminum has a simple Fermi surface, without deformations of type (B) or (C). The distribution of b^2 is appropriately narrower, and the average value $\langle b^2\rangle \approx 3.4 \times 10^{-7}$ is about 50 times smaller than for trivalent aluminum. Adjusting for the density of states (monovalent aluminum would have $1/\tau$ reduced $\sim 1/3^{1/3}$ times) the spin relaxation would be about 70 times slower. These values may somewhat vary for different scattering processes.

How different spin hot spots contribute to the renormalization of $\langle b^2\rangle$ becomes clear from Fig. 3, which plots what we call the *average density of bands* (ADOB). ADOB is the Fermi surface average of the number of (vertical) bands in the interval $(\Delta, \Delta + d\Delta)$: $\mathrm{ADOB}(\Delta) = (1/g_F)\sum_{\mathbf{k},n\neq m} \delta(\tilde{E}_{\mathbf{k}n} - E_F)\delta(|\tilde{E}_{\mathbf{k}m} - E_F| - \Delta)$, were band energies $\tilde{E}_{\mathbf{k}n}$ are computed without the spin-orbit interaction, and g_F is the density of states (per spin) at E_F.

The average $\langle b^2\rangle$ can then be well approximated by taking the integral (from zero to infinity) of ADOB weighted by the mixing factor $(1 - \Delta/\sqrt{\Delta^2 + 4V_{\mathrm{SO}}^2})/2$. Figure 3 uses $V_{\mathrm{SO}} = 1.1 \times 10^{-4}$ a.u., the value that gives the right answer for $\langle b^2\rangle$. At small Δ ADOB is linear. This is expected for a region around R where band gaps increase linearly with increasing distance from R [20]. The linear increase (see also Table I) continues up to the point where the Fermi surface crosses the first ($\Delta \approx 2V_1$) and the second ($\Delta \approx 2V_2$) closest BZ boundary plane. At these points, ADOB has power-law singularities (Table I). Larger band separations, where ADOB develops either logarithmic or steplike singularities [21], are irrelevant. Indeed, the cumulative average $\langle b^2\rangle(\Delta)$ saturates after the second peak so that $\langle b^2\rangle$ is almost entirely determined by the regions close to accidental degeneracies and BZ boundaries. As Fig. 3 shows, these regions contribute about equally to $\langle b^2\rangle$. The behavior of $\langle b^2\rangle(\Delta)$ also shows that states in the immediate neighborhood of R (the red spots in Fig. 2) with $\Delta \lesssim 2V_{\mathrm{SO}} \approx 2.2 \times 10^{-4}$ are statistically irrelevant. It is rather a broader neighborhood of R [the states with $2V_{\mathrm{SO}} \lesssim \Delta \lesssim 2V_1$ and estimate (B)] that is contributing most. These findings are confirmed by the analytical calculation reported in Table I.

Table I summarizes our estimates of ADOB and $\langle b^2\rangle$ for three different cases. The estimates were obtained analytically by the orthogonalized-plane-wave methods developed in Ref. [20]. If the Fermi surface (in an extended zone) lies entirely within the first BZ (region I, alkali and noble metals), the enhancement of $\langle b^2\rangle$ is about tenfold since $E_{\min} \approx 0.1$. If the Fermi surface crosses a zone boundary (region II, polyvalent metals), the enhancement is $\sim 1/V_{\mathbf{G}}$, typically a hundred. Relative to I, however, the enhancement is in units of ten, in agreement with the numerical calculation. Qualitatively, a fraction of $\sim V_{\mathbf{G}}$ states on the Fermi surface comes close to zone boundaries ($\Delta \approx 2V_{\mathbf{G}}$) so that their $|b_{\mathbf{k}n}|^2 \sim (V_{\mathrm{SO}}/V_{\mathbf{G}})^2$. The contribution

TABLE I. Estimated contributions of different Fermi surface regions to ADOB and $\langle b^2 \rangle$. (I) The Fermi surface is entirely within the first BZ, crosses (II) a zone boundary, and (III) an accidental degeneracy line at R. Momentum and energy are measured in the units of $G/2$ and $(G/2)^2/2$, respectively. The region III assumes an fcc lattice with period a, energy and momentum in the units of $2\pi/a$ and $(2\pi/a)^2/2$, respectively, and $V_2 \gg V_1 \gg V_2^2$. Both ADOB and $\langle b^2 \rangle$ come with the corresponding multiplicative factor. Notation: $k_F = \sqrt{E_F}$ is the Fermi vector, $E_{\min} = G(G - 2k_F)$ is the band gap at the point of closest approach to the BZ plane given by $\mathbf{G}$; N_G and N_R are the numbers of the corresponding BZ planes and accidental degeneracy points ($N_R = 24$); Θ is the step function.

FS area	Multiplicative factor	ADOB	b^2/V_{SO}^2
I	$N_G/4Gk_F$	$\Theta(\Delta - E_{\min})$	$1/E_{\min}$
II	$N_G/4Gk_F$	$\Delta/\sqrt{\Delta^2 - 4V_{\mathbf{G}}^2}$	$(\pi/4)(1/V_{\mathbf{G}})$
III	$N_R/8k_F$	$(V_2/V_1)^2\Delta$	$(V_2/V_1)^2 \ln(V_1/V_{\mathrm{SO}})$

of these points to $\langle b^2 \rangle$ is therefore $\sim V_{\mathbf{G}} \times (V_{\mathrm{SO}}/V_{\mathbf{G}})^2$; the enhancement is $\sim 1/V_{\mathbf{G}}$, consistent with the result in Table I. Curiously, the region II applies also to the noble metals, whose Fermi surfaces touch zone boundaries [12]. This effect is, however, masked by the unusually high $V_{\mathbf{G}}$ for these metals [22] ($V_{\mathbf{G}} \approx E_{\min}$, otherwise the Fermi surface would not touch the zone planes). The enhancement of $\langle b^2 \rangle$ can be also significant if the Fermi surface crosses a line of accidental degeneracy (region III). Indeed, by substituting the values for aluminum, the enhancement is about tenfold, similar to case (II), again agreeing with the numerical result. Finally, not shown in Table I is the case when E_F coincides with a degenerate level at a special symmetry point. Such a situation occurs, for example, in Pd and Pt, whose Fermi surfaces go through the fcc L point. If the spin-orbit interaction lifts this degeneracy, the renormalization of $\langle b^2 \rangle$ can be significant (we find the enhancement $\sim V_{\mathbf{G}}/V_{\mathrm{SO}}$ for the fcc W point [21]).

Our final note concerns the hexagonal Mg and Be, where the deviation of T_1 from the main group is most striking [10]. We argue that this is also a manifestation of the band renormalization of c^2. Without the spin-orbit interaction, all of the states at the hexagonal faces of the first BZ of a simple hexagonal structure are degenerate [12]. The spin-orbit interaction lifts this degeneracy [8] (except at some symmetry points and lines), presumably by the amount $V_{\mathbf{G}}V_{\mathrm{SO}}$, the largest second-order term containing the spin-orbit interaction (any first-order term vanishes since the structure factor associated with the hexagonal faces is zero [12]). The contribution to $\langle b^2 \rangle$ of the points where the Fermi surface intersects the hexagonal faces is $\sim V_{\mathbf{G}}V_{\mathrm{SO}}$ (in the units of Table I): the characteristic value $|b_{\mathbf{k}n}|^2 \sim 1$, times the area of the affected part of the Fermi surface, $V_{\mathbf{G}}V_{\mathrm{SO}}$. The enhancement measured in terms of V_{SO}^2 is then $V_{\mathbf{G}}/V_{\mathrm{SO}}$; this can be as large as a thousand for light elements such as Mg and Be.

We acknowledge discussions with P. B. Allen and M. Johnson. This work was supported by the U.S. ONR.

Note added.—After submission of our work R. H. Silsbee brought to our attention an earlier paper [23] which suggests the importance of the accidental degeneracy points for the spin relaxation in aluminum.

[1] M. Johnson, Science **260**, 320 (1993); J. Magn. Magn. Mater. **140–144**, 21 (1995); **156**, 321 (1996); Mater. Sci. Eng. B **31**, 199 (1995).
[2] G. Prinz, Phys. Today **48**, No. 4, 58 (1995).
[3] J. M. Kikkawa, I. P. Smorchkova, N. Samarth, and D. D. Awschalom, Science **277**, 1284 (1997); J. M. Kikkawa and D. D. Awschalom, Phys. Rev. Lett. **80**, 4313 (1998).
[4] D. P. DiVincenzo, Science **270**, 255 (1995).
[5] G. Feher and A. F. Kip, Phys. Rev. **98**, 337 (1955).
[6] M. Johnson and R. H. Silsbee, Phys. Rev. Lett. **55**, 1790 (1985); Phys. Rev. B **37**, 5326 (1988).
[7] The longitudinal "spin-lattice" relaxation time T_1 equals, at least for cubic metals, the transverse "dephasing" relaxation time T_2, as shown in D. Pines and C. P. Slichter, Phys. Rev. **100**, 1014 (1955).
[8] R. J. Elliott, Phys. Rev. **96**, 266 (1954).
[9] Y. Yafet, in *Solid State Physics*, edited by F. Seitz and D. Turnbull (Academic, New York, 1963), Vol. 14.
[10] P. Monod and F. Beuneu, Phys. Rev. B **19**, 911 (1979); F. Beuneu and P. Monod, Phys. Rev. B **18**, 2422 (1978).
[11] Extrapolated from the experimental data in Ref. [6] and S. Schultz, G. Dunifer, and C. Latham, Phys. Lett. **23**, 192 (1966); D. Lubzens and S. Schultz, Phys. Rev. Lett. **36**, 1104 (1976).
[12] N. W. Ashcroft and N. D. Mermin, *Solid State Physics* (Saunders, New York, 1976).
[13] F. Vescial, N. S. Vander Ven, and R. T. Schumacher, Phys. Rev. **134**, A1286 (1964); W. Kolbe, Phys. Rev. B **3**, 320 (1971).
[14] P. B. Allen, Phys. Rev. B **36**, 2920 (1987).
[15] A. W. Overhauser, Phys. Rev. **89**, 689 (1953).
[16] D. R. Mašović and S. Zeković, Phys. Status Solidi (b) **89**, K57 (1978); V. Veljković and I. Slavić, Phys. Rev. Lett. **29**, 105 (1972).
[17] N. W. Ashcroft, Philos. Mag. **8**, 2055 (1963).
[18] G. B. Bachelet, D. R. Hamann, and M. Schlüter, Phys. Rev. B **26**, 4199 (1982).
[19] P. B. Allen, Phys. Status Solidi (b) **120**, 529 (1983).
[20] W. A. Harrison, *Pseudopotentials in the Theory of Metals* (Benjamin, New York, 1966).
[21] J. Fabian and S. Das Sarma (unpublished).
[22] M. L. Cohen and V. Heine, in *Solid State Physics*, edited by H. Ehrenreich, F. Seitz, and D. Turnbull (Academic, New York, 1970), Vol. 24, p. 183.
[23] R. H. Silsbee and F. Beuneu, Phys. Rev. B **27**, 2682 (1983).